Biomedicine & Pharmacotherapy 154 (2022) 113597

Contents lists available at ScienceDirect

Biomedicine & Pharmacotherapy

journal homepage: www.elsevier.com/locate/biopha

Establishment of a direct 2.5D organoid culture model using companion animal cancer tissues

Amira Abugomaa [a,b], Mohamed Elbadawy [a,c,*], Haru Yamamoto [a], Hiromi Ayame [a], Yusuke Ishihara [a], Yomogi Sato [a], Hideyuki Yamawaki [d], Masahiro Kaneda [e], Tatsuya Usui [a,**], Kazuaki Sasaki [a]

[a] Laboratory of Veterinary Pharmacology, Department of Veterinary Medicine, Faculty of Agriculture, Tokyo University of Agriculture and Technology, 3-5-8 Saiwai-cho, Fuchu, Tokyo 183-8509, Japan

[b] Faculty of Veterinary Medicine, Mansoura University, 35516 Mansoura, Egypt

[c] Department of Pharmacology, Faculty of Veterinary Medicine, Benha University, Moshtohor, 13736 Toukh, Egypt

[d] Laboratory of Veterinary Pharmacology, School of Veterinary Medicine, Kitasato University, 35-1 Higashi 23 ban-cho, Towada, Aomori 034-8628, Japan

[e] Laboratory of Veterinary Anatomy, Department of Veterinary Medicine, Faculty of Agriculture, Tokyo University of Agriculture and Technology, 3-5-8 Saiwai-cho, Fuchu, Tokyo 183-8509, Japan

ARTICLE INFO

Keywords:
2.5D
3D
Cats
Culture model
Dogs
Organoids
Patient-derived
Primary

ABSTRACT

Like humans, cancer affects companion animals with similar genetic risks and incident rates. To improve treatment strategies for pet cancers, new research models are necessary. Patient-derived 3D organoid culture models are valuable and ensure the development of new effective therapies. In the previous study, we established a 3D organoid-derived 2.5D organoid culture model that recapitulated some characteristics of their parental 3D organoids. In the present study, we aimed to generate a 2.5D organoid culture model directly from cancer-diseased dogs and cats using special 2.5D media. The primary cultured cells in 2.5D media (direct 2.5D organoids) showed better attachment, growth, marker expression, and faster proliferation speed than those cultured in normal Dulbecco's Modified Eagle Medium media. The direct 2.5D organoids showed expression of each specific marker to their original cancer tissues and exhibited tumorigenesis *in vivo*. Moreover, the direct 2.5D organoids exhibited concentration-dependent responses to anti-cancer drugs, and different sensitivity profiles were shown among the strains. Our data suggest that the direct 2.5D organoid culture model might become a useful tool beyond 2D cell lines to study cancer biology in companion animals and could provide new platforms for screening the anti-cancer drugs.

1. Introduction

Like humans, pets can be affected by neoplasia, whose genetic risks are similar to humans [1]. The incident rate of cancers in dogs is roughly the same as in humans but higher than in cats. According to the American Veterinary Medical Association, aging in dogs and cats causes an upsurge in cancer onset. Almost half of the dogs over 10 years old will suffer from cancer, which causes about 50 % of deaths. Dogs suffer from a variety of cancers, and the most common is skin cancer. Other dog cancers include bladder cancer, prostate cancer, lymphoma, oral carcinoma, mammary, and abdominal tumors [2–4]. Veterinarians need continually to tailor treatment dosages to optimize efficacy and minimize side effects [2]. Treatment options for cancer in dogs and cats are similar to those in humans and depend on cancer type, clinical stage, and associated risk factors [5]. They include surgery, radiotherapy, chemotherapy, and immunotherapy.

To improve treatment strategies for pet cancers, new research models are necessary. Many *in vitro* studies have been performed with immortalized cancer cell lines using a 2D culture system. Although it is easily processed, it has several drawbacks, such as limitations for certain individuals, less cell-cell adhesion, and less cellular heterogeneity. These problems make it different from the tumor microenvironment [6]. Further, not all primary tissue samples can be developed into cell lines. For example, among 189 human breast cancer samples, only 21 cell lines

* Correspondence to: Department of Pharmacology, Faculty of Veterinary Medicine, Benha University, Moshtohor, 13736 Toukh, Elqaliobiya, Egypt.
** Corresponding author.
E-mail addresses: Mohamed.elbadawy@fvtm.bu.edu.eg (M. Elbadawy), fu7085@go.tuat.ac.jp (T. Usui).

https://doi.org/10.1016/j.biopha.2022.113597
Received 3 July 2022; Received in revised form 10 August 2022; Accepted 19 August 2022
Available online 26 August 2022

Table 1
Sample information.

Case ID	Age (year old)	Breed	Sex	Sampling Date	Prior Therapy	Other information
DBC21047	13	Italian Greyhound	Male (castrated)	11/29/2021	Lapatinib, Toceranib, Firocoxib, Prednisolone	This sample was used as dog bladder cancer 1 (Figs. 1, 2, 3, and 4).
DBC21039	9	Miniature Dachshund	female	10/23/2021	Carboplatin	This sample was used as dog bladder cancer 2 (Fig. 4).
DMT21006	12	Pomeranian	female	11/21/2021	None	This sample was used as dog mammary tumor 1 (Figs. 1, 2, 3, 4, and 5).
DMT21005	10	Mix	female (spayed)	11/1/2021	None	This sample was used as dog mammary tumor 2 (Fig. 4).
DLC21004	15	Shih Tzu	Male (castrated)	8/31/2021	None	This sample was used as dog lung cancer (Figs. 1, 3, and 5).
CMT21011	13	Egyptian Mau	female (spayed)	10/11/2021	None	This sample was used as cat mammary tumor (Figs. 1, 3, and 5).
CST21004	16	Mix	female (spayed)	10/26/2021	None	This sample was used as cat skin tumor (Figs. 1, 2, and 3).
DM21004	12	Toy poodle	female (spayed)	10/26/2021	None	This sample was used as dog melanoma (Figs. 1, 2, and 3).

were established [7].

Recently, researchers have developed a 3D organoid culture model to overcome these limitations. Organoids could recapitulate the cellular heterogeneity of the microenvironment, functions, and molecular imprints of their parental tissues [8,9]. Therefore, organoid research revealed a great promise in medical and translational research to develop new personalized therapies, especially for cancer biology [10,11], disease model [8,12], and analysis of drug resistance [13–18].

Despite these advantages of organoids, the culture method meets significant challenges. For example, Matrigel used in 3D culture is derived from animals with undefined hydrogel matrix compositions besides its expensive cost. In addition, it takes a long processing time for culturing and growing organoids. Therefore, some researchers have focused on improving the 2D culture systems to overcome these limitations [19–21]. Recently, Puca et al. isolated 2D cells from prostate organoids and called them 2D organoids because it kept the purity and genomic imprint of their parental 3D organoids and the original tumor tissues [20]. Additionally, Shamir et al. found that the 2.5D organoids grown on the surface of a thick layer of Matrigel showed tissue-specific differentiation of various cells [21].

In the previous study, we induced the migration of cells from the 3D organoids to the surface of the culture plate using a special 2.5D medium. Our established 3D organoid-derived 2.5D organoids could recapitulate some characteristics of their parental 3D organoids [19]. This model was different from the previous two models regarding the lesser cost, shorter processing time, and easier processing. However, 3D organoids are necessary at first to generate it.

To date, 2.5D media were not used to culture primary cancer cells. Therefore, in the present study, we have established a new 2.5D organoid culture system directly (without the need for 3D organoids as in the previous study) from different animal cancer tissues and urine.

2. Materials and methods

2.1. Materials

To generate direct 2.5D organoids from companion animal cancer tissues, we used special 2.5D organoid media described in the previous study [19]. The 2.5D medium components were as follows: Advanced Dulbecco's Modified Eagle's Medium (DMEM)/F12 (Thermo Fisher Scientific Inc., Waltham, MA, USA) supplemented with 1 % GlutaMax (Thermo Fisher Scientific Inc), 10 mM 4-(2-hydroxyethyl)− 1-piperazine ethanesulfonic acid (HEPES; WAKO, Osaka, Japan), 1 mM N-acetyl-L-cysteine (Sigma-Aldrich), 10 mM Nicotinamide (Sigma-Aldrich, St. Louis, MO, USA), 0.5 μM A83-01 (Adooq Bioscience, Irvine, CA, USA), 50 ng/ml epidermal growth factor (EGF) (Thermo Fisher Scientific Inc.), 1 % penicillin-streptomycin (PS; WAKO), and 5 % fetal bovine serum (FBS; Thermo Fisher Scientific Inc.). The used antibodies to characterize the cell components were as follows: UPK3A and CK20 (Bioss, Woburn, MA, USA), CK5 (GeneTex, Inc., Irvine, CA, USA), CK7 and TTF1 (Santa Cruz Biotechnology, Dallas, TX, USA), Melan A (Leica Biosystems, Newcastle, UK), Progesterone (Invitrogen, Waltham, MA, USA), Estrogen (Abcam, Cambridge, MA, USA), and HER2 (Enogene, NY, USA). Fluorescent secondary antibodies were as follows: Alexa Fluor 488 goat anti-rabbit IgG and Alexa Fluor 488 goat anti-mouse IgG; (Thermo Fisher Scientific Inc.). Dako Envision+dual Link System-HRP (Agilent Technologies Inc., Santa Clara, CA, USA). Anti-cancer drugs were as follows: vinblastine, mitoxantrone, vinorelbine, and doxorubicin (Cayman Chemical, Ann Arbor, MI, USA), toceranib (Sigma-Aldrich), and cisplatin and carboplatin (Fuji Film Wako Pure Chemical Co., Osaka, Japan).

2.2. Generation of direct 2.5D organoids

In the previous study, we generated urine sample-derived dog bladder cancer 3D organoids [22]. From this bladder cancer organoid, we generated 2.5D organoids by inducing the migration of cells using special 2.5D media [19]. In the present study, we challenged the 2.5D media to generate 2.5D organoids directly. Urine samples from bladder cancer diseased dogs, tissue samples from dog mammary tumors, melanoma, lung adenocarcinoma, cat skin tumor, and mammary tumors were used. All samples were collected in 2021 from animal clinics in Japan (animal information is listed in Table 1) and transferred rapidly to our laboratory in the preservation buffer. The study was conducted after getting written informed consent from animal owners and under the direction of the Institute Animal Care and Use Committee of Tokyo University of Agriculture and Technology approval (Approval number: 0020007). Urine samples from bladder cancer diseased dogs were washed with sterilized phosphate-buffered saline (PBS) and trypsinized by TrypLE Express solution (Thermo Fisher Scientific Inc.) at 37 °C for 5 min. After that, the cells were strained through 70 μM nylon cell strainers and seeded. Solid tumor samples were properly minced by microsurgical scissors into fine pieces in a 6 cm-Petri dish on ice under aseptic conditions. After that, they were transferred to 15 ml tubes containing prewarmed (at 37 °C) advanced DMEM media with 0.125 mg/ml of both collagenase type I and II (LiberaseTH, Roche Diagnostics, Germany). The tubes were then incubated in a shaking water bath at 37 °C for 30 min and were pipetted every 15 min to allow tissue digestion and cell release. After the tubes were trypsinized at 37 °C for 5 min, the cell solutions were passed through 70 μm cell strainers. The cell pellets were cultured in 2.5D organoid media or 2D epithelial cell line media (normal DMEM containing 10 % FBS and 1 %

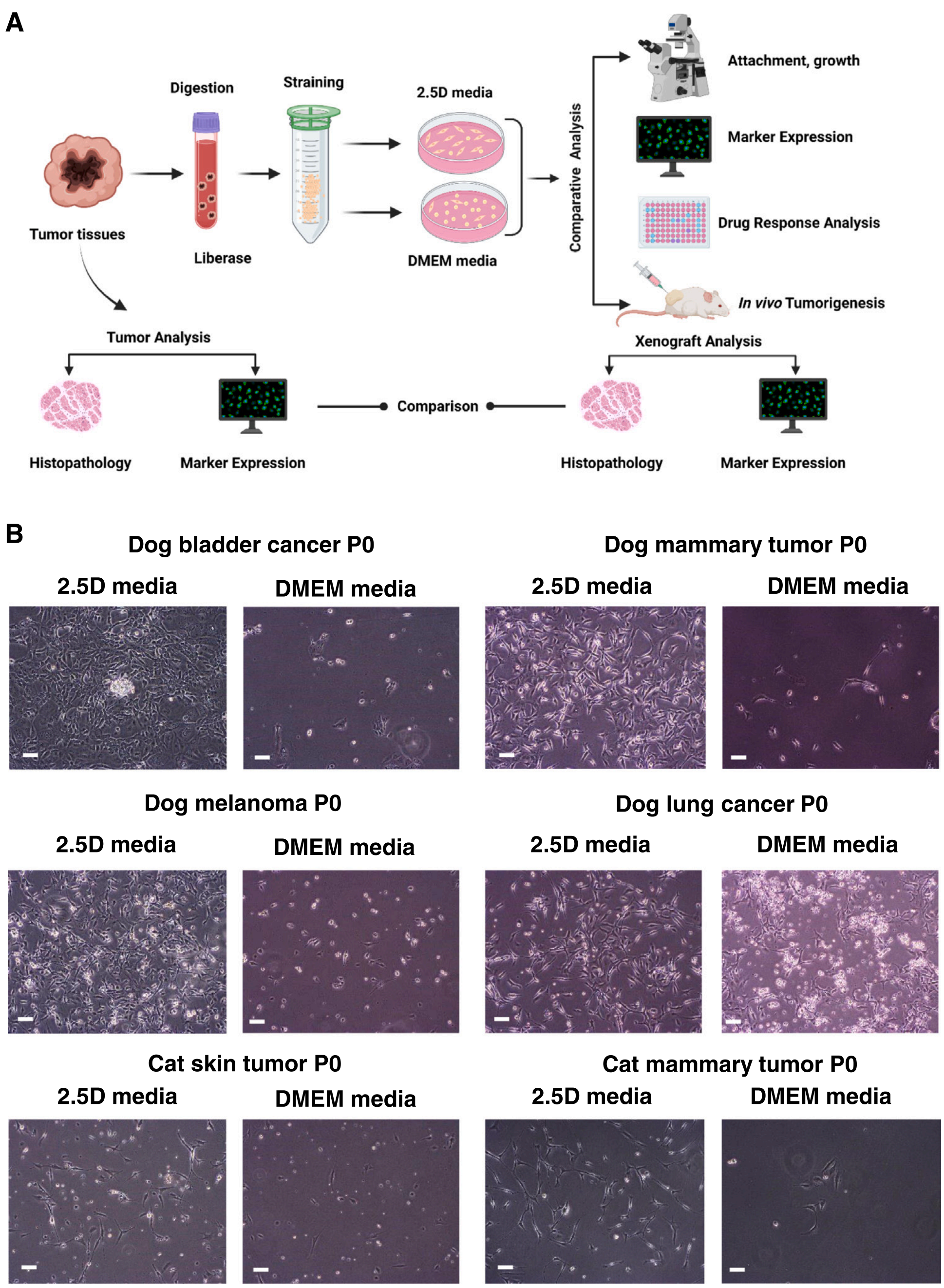

Fig. 1. Schematic diagram of generation of direct 2.5D organoid cells using special 2.5D organoid media (A). After cutting and digesting the tissue sample, the solution was strained. The obtained cells were seeded in 2.5D organoid media (2.5D media) or normal DMEM media. The attachment and proliferation speeds of cells were compared. Thereafter, the cells grown in the 2.5D media underwent analysis for marker expression, drug response, and *in vivo* tumorigenesis. The xenografts were compared with the original tumor using H&E staining and marker expression. Comparison of cell attachment of different cancer cells from dogs and cats in the 2.5D and normal DMEM media (B). Representative bright-field comparative images were taken after 7–14 days. Scale bar: 200 μm.

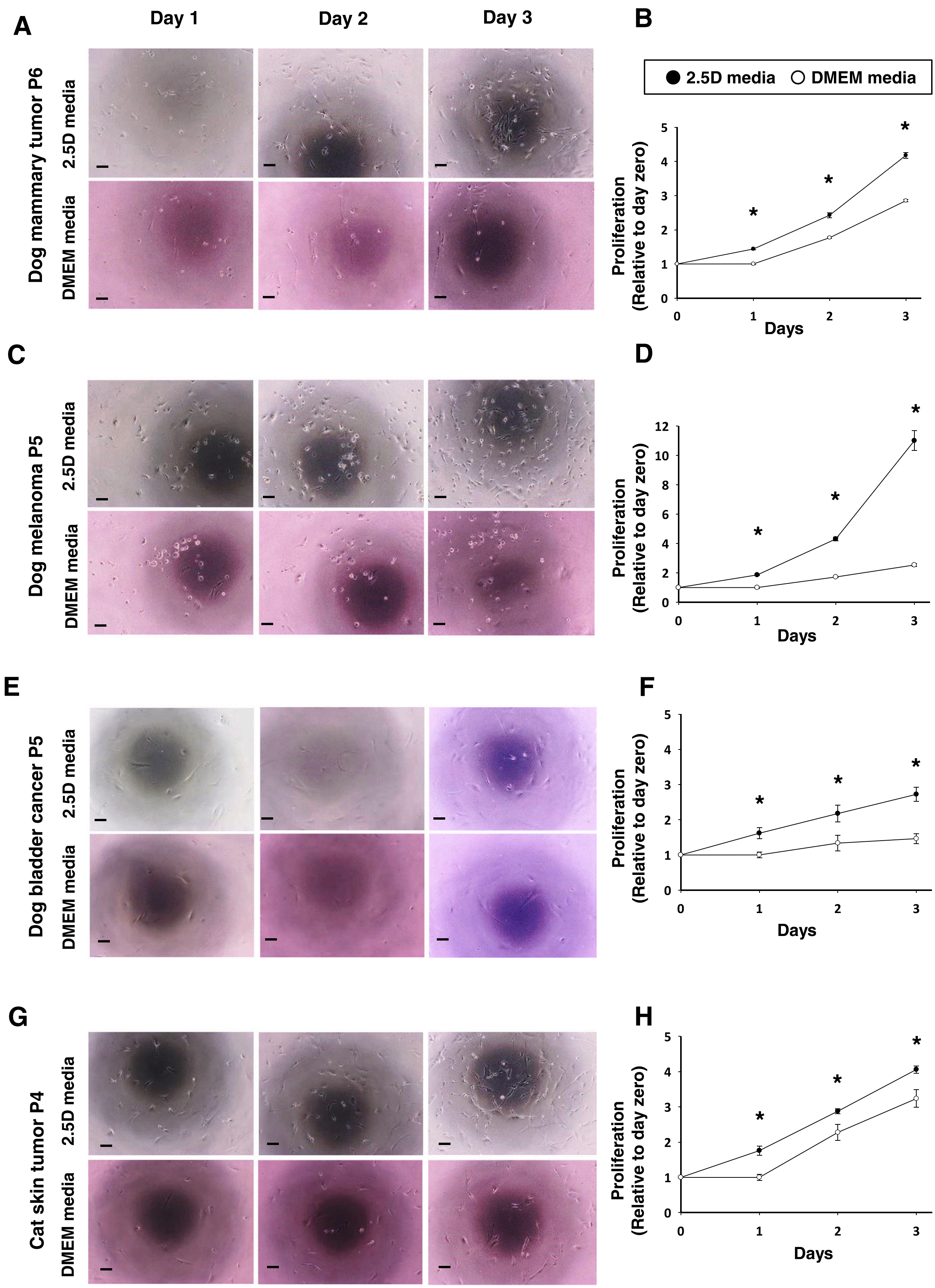

Fig. 2. Comparison of cell proliferation capacity between 2.5D and normal DMEM media. After an equal number of cells (1×10^3 cells/well) was seeded in a 96-well plate, the number of living cells was evaluated on days 1, 2, and 3 after seeding. Representative bright-field images of cell proliferation on days 1, 2, and 3 of dog mammary tumor (A), dog melanoma (C), dog bladder cancer (E), and cat skin tumor cells (E) seeded in 2.5D or normal DMEM media. Scale bar: 200 µm. Analysis of the cell proliferation on days 1, 2, and 3 between 2.5D and normal DMEM media as assayed by Prestoblue cell viability reagent and the results were shown as a fold increase relative to day zero represented by the value one at Y-axis (B, D, F, H, n = 6). Data were expressed as mean ± S.E.M. *$P < 0.05$ *vs.* DMEM media.

Table 2
Statistical parameters of cell proliferation speed in 2.5D media at day 1, 2, and 3.

Parameters	*P*-value			DF Total (Between groups+ residual)			F-value			t-value		
	Day 1	Day2	Day3	Day 1	Day2	Day3	Day 1	Day2	Day3	Day 1	Day2	Day3
Canine mammary tumor	<0.001	<0.001	<0.001	11 (1 + 10)	11(1 + 10)	11(1 + 10)	140.318	78.149	218.124	11.846	8.84	14.769
Dog melanoma	<0.001	<0.001	0.004	11 (1 + 10)	11(1 + 10)	11(1 + 10)	177.578	412.661	154.541	13.326	20.314	12.431
Dog bladder cancer	0.005	0.037	0.002	11 (1 + 10)	8 (1 + 7)	9 (1 + 8)	12.492	6.617	21.12	3.534	2.572	4.596
Cat skin tumor	<0.001	0.03	0.012	11 (1 + 10)	11(1 + 10)	8 (1 + 7)	23.351	6.393	11.226	4.832	2.528	3.35
Cat mammary tumor	<0.001	<0.001	<0.001	11 (1 + 10)	11 (1 + 10)	11 (1 + 10)	455.112	364.11	93.116	21.334	19.082	9.65
Dog lung cancer	<0.001	<0.001	<0.001	11 (1 + 10)	11 (1 + 10)	11 (1 + 10)	23.598	305.666	107.801	4.858	17.483	10.383

DF: degrees of freedom

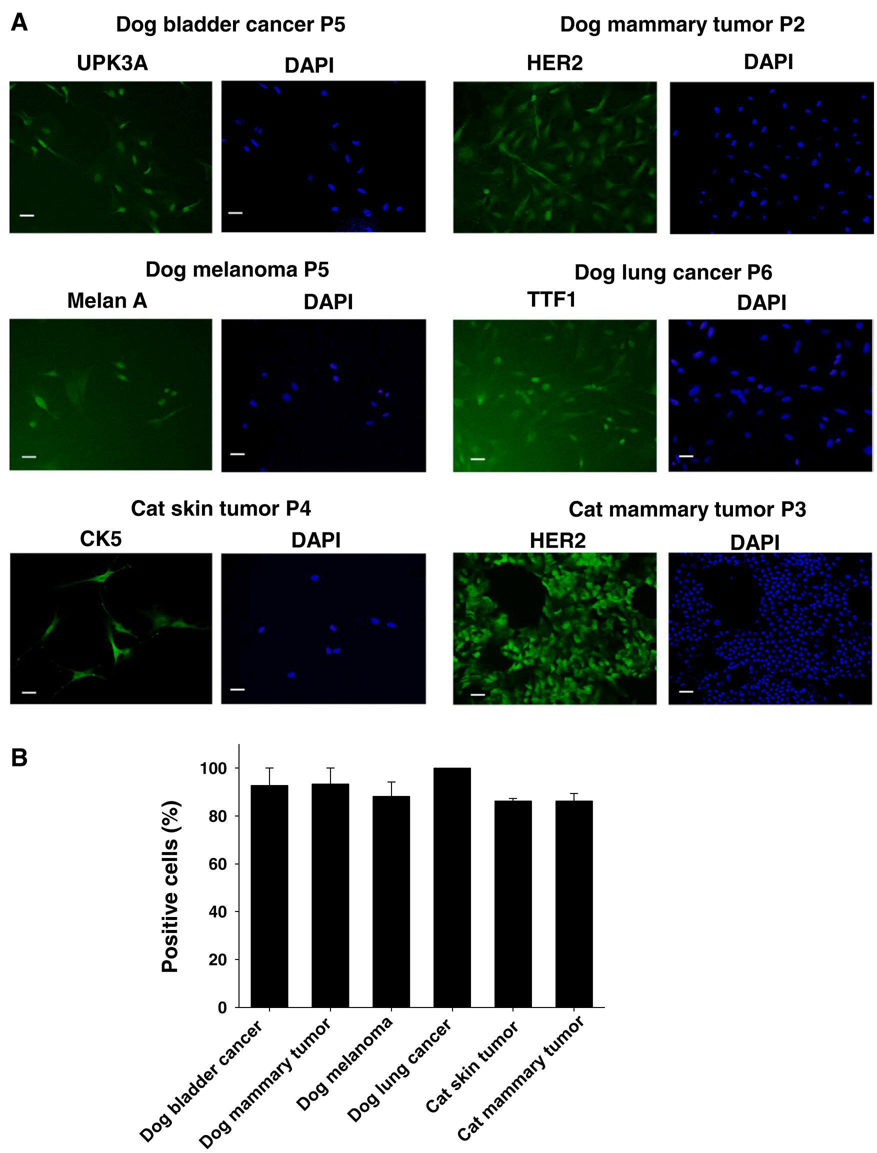

Fig. 3. Characterization of the cells cultured in 2.5D media. Expression of a urothelial cell marker, UPK3A, a mammary cell marker, HER2, a melanocyte marker, Melan A, a lung adenocarcinoma cell marker, TTF1, and a basal cell marker, CK5 in six kinds of cultured cells in 2.5D media (A). Scale bar: 100 µm. Quantification of marker expression in the stained cells *vs.* DAPI as analyzed by ImageJ software (B, n = 3). Results were expressed as mean ± S.E.M.

penicillin-streptomycin (PS)) at 37 °C in a CO_2 incubator.

2.3. Passaging of direct 2.5D organoids

After 70–80 % confluent conditions, the cells were passaged into a new 6 cm-dish at a proportion of 1:3–4. Briefly, 1 ml of 5 mM ethylenediaminetetraacetic acid (EDTA)/PBS was added to the 6 cm-culture dish, and the dish was placed in a CO_2 incubator at 37 °C for 10 min to detach the cells. After that, the solutions were collected into 15 ml tubes. Subsequently, 1 ml of TrypLE was added, and the dishes were incubated at 37 °C for 3–5 min to dissociate the cells. Collected cell pellets were mixed with new 2.5D organoid media or normal DMEM media and seeded into new 6 cm dishes.

Table 3
Quantification of marker expression in different 2.5D cells after immunofluorescence.

UPK3A in BC cells				CK5 in canine mammary tumor cells				Melan A in dog melanoma cells				CK5 in feline skin tumor cells				HER2 in Feline mammary tumor cells				TTF1 in Dog lung cancer cells			
	DAPI	FITC	Positive cell (%)		DAPI	FITC	Positive cell (%)		DAPI	FITC	Positive cell (%)		DAPI	FITC	Positive cell (%)		DAPI	FITC	Positive cell (%)		DAPI	FITC	Positive cell (%)
Image 1	23	23	100	Image 1	15	12	80	Image 1	15	12	80	Image 1	4	4	100	Image 1	640	544	85	Image 1	62	57	91.9
Image 2	23	18	78.3	Image 2	15	15	100	Image 2	13	11	84.62	Image 2	8	8	100	Image 2	612	540	88.2	Image 2	28	24	85.7
Image 3	11	11	100	Image 3	12	12	100	Image 3	12	12	100	Image 3	8	8	100	Image 3	670	573	85.5	Image 3	74	60	81.1
Average	19	17.3	92.8	Average	14	13	93.3	Average	13.3	11.7	88.2	Average	6.67	6.67	100	Average	640.67	552.3	86.3	Average	54.7	47	86.2
SD	6.93	6.03	12.6	SD	1.73	1.73	11.5	SD	1.53	0.577	10.47	SD	2.31	2.31	0	SD	29.01	18.0	1.74	STDEV	23.9	19.97	5.45
S.E.M	4.00	3.48	7.25	S.E.M	1.00	1.00	6.67	S.E.M	0.882	0.333	6.05	S.E.M	1.33	1.33	0	S.E.M	16.75	10.40	1.00	S.E.M	13.8	11.5	3.14

2.4. *Comparison of culture efficiency between direct 2.5D organoid media and normal DMEM media*

After isolation of the cells, they were equally seeded in 2.5D organoid media or normal DMEM media for three days, and the efficiency of cell attachment and growth was compared. Representative bright-field images were captured using a light microscope (CKX-53; Olympus, Tokyo, Japan).

2.5. *Cell proliferation assay*

After an equal number of cells was seeded in a 96-well plate at a density of 1×10^3 cells/well, each cell was cultured for three days. The number of living cells on days 1, 2, and 3 was evaluated with Prestoblue™ Cell Viability Reagent (Thermo Fisher Scientific Inc.). The fluorescence intensity was measured with a microplate reader (TECAN, Seestrasse, Switzerland) at an excitation wavelength of 560 nm and an emission of 590 nm. Representative bright-field images were captured using a light microscope (CKX-53; Olympus, Tokyo, Japan). The data were graphed and analyzed using the SigmaPlot software (V 14.5, Systat Software Inc, IL, USA).

2.6. *Confirmation of marker expressions by immunofluorescence staining*

To check the potential of the 2.5D organoids in recapitulating the patient's tissue cellular components, immunofluorescence staining with specific markers was performed in four strains at early and late passages as described previously [11,19,22]. Further, in two strains, the difference in the marker expression between 2.5D medium and DMEM was evaluated. Briefly, 2×10^5 cells /well were seeded on a coverslip in 12-well plates. After 75 % confluent condition, the cells on the coverslips were fixed with a 4 % paraformaldehyde (PFA) solution for 15 min at room temperature (RT). The cells were then washed with PBS, treated with 0.2 % Triton-X/PBS, and shaken for a few seconds. Thereafter, the blocking was carried out by using 1.5 % normal goat serum/PBS for 30 min at RT. Subsequently, the cells were treated with primary antibodies (UPK3A; 1:200, CK5; 1:100, Melan A; 1:100, TTF1; 1:100, Progesterone; 1:100, Estrogen; 1:100, and HER2; 1:200) and kept overnight at 4 °C. After they were treated with the secondary antibodies (1:500) and DAPI solution (1:1000) for 1 h at RT, they were observed using a fluorescence microscope (BX61, Olympus, Tokyo, Japan). Several images were captured from different fields and quantified by ImageJ densitometry analysis software (National Institutes of Health, Bethesda, MD, USA).

2.7. *Drug sensitivity test of direct 2.5D organoids*

The sensitivity of direct 2.5D organoids to anti-cancer drugs was analyzed as described previously [11,19,23]. Briefly, 1×10^3 cells were seeded in 96-well plates and incubated for 24 h. The cells were then treated with different anti-cancer drugs including a microtubule inhibitor, vinblastine (0.1–10 nM) or vinorelbine (0.01–10 μM), a topoisomerase inhibitor, mitoxantrone (1–100 ng/ml), or doxorubicin (1–100 ng/ml), a tyrosine kinase inhibitor, toceranib (2–8 μM), or a DNA-damaging agent, carboplatin (1–100 μg/ml) or cisplatin (0.1–100 μM) for 72 h. The concentrations of these drugs were determined based on their blood therapeutic level in the clinic and pharmacokinetic data [24–27]. Cell viabilities were evaluated similarly as in the cell proliferation assay.

2.8. *Tumorigenic potential of direct 2.5D organoids*

The tumorigenic potential of direct 2.5D organoids was assessed as described before [19,28]. Six-week-old male immunodeficient mice (C.B-17/IcrHsd-*Prkdc*^{scid}) were obtained from Japan SLC (Shizuoka, Japan) and housed under specific pathogen-free conditions. To check the tumorigenic potentials of the generated 2.5D organoids, 1×10^6 cells

Table 4
Quantification for difference of specific marker expression between 2.5D and DMEM.

2.5D UPK3A in BC cells				Progesterone in canine mammary tumor cells				HER2 in canine mammary tumor cells			
	Dapi	FITC	Positive cell (%)		Dapi	FITC	Positive cell (%)		Dapi	FITC	Positive cell (%)
Image 1	23	23	100	Image 1	82	75	91.46341	Image 1	41	37	90.2439
Image 2	23	18	78.3	Image 2	46	41	89.1	Image 2	68	58	85.29
Image 3	11	11	100	Image 3	81	70	86.41975	Image 3	47	39	82.97872
Average	19	17.3	92.8	Average	69.66667	62.0	89.0	Average	52.0	44.7	86.2
SD	6.93	6.03	12.6	SD	20.50	18.36	2.5	SD	14.18	11.590	3.71
S.E.M	4.00	3.48	7.25	S.E.M	11.84	10.60	1.46	S.E.M	8.185	6.692	2.14
DMEM											
Image 1	21	6	28.57143	Image 1	46	18	39.13043	Image 1	18	7	38.88889
Image 2	28	3	10.7	Image 2	19	8	42.10526	Image 2	8	3	37.50
Image 3	33	13	39.39394	Image 3	15	7	46.66667	Image 3	11	6	54.54545
Average	27.33333	7.3	26.2	Average	26.66667	11	42.6	Average	12.3	5.3	43.6
SD	6.03	5.13	14.5	SD	16.86	6.08	3.8	SD	5.13	2.082	9.47
S.E.M	3.48	2.96	8.36	S.E.M	9.74	3.51	2.19	S.E.M	2.963	1.202	5.47
Statistical parameters of quantification for difference of specific marker expression 2.5D and DMEM											
Parameters	*P*-value	DF Total (Between groups+ residual)	F-value	t-value							
Dog bladder cancer (UPK3A)	<0.004	5 (1 + 4)	36.204	6.17							
Canine mammary tumor (Progesterone)	<0.001	5 (1 + 4)	310.343	17.671							
Cat mammary tumor (HER2)	<0.002	5 (1 + 4)	52.481	7.244							

were implanted subcutaneously into the back of mice. Six weeks later, the 2.5D organoid-derived tumor tissues were dissected under isoflurane anesthesia and used for H&E and immunohistochemical staining. All animal experiments in the present study were performed following the Guide to Animal Use and Care of Tokyo University of Agriculture and Technology and approved by the ethics committee (Approval number: R03-85).

2.9. Histopathological and immunohistochemical examination of 2.5D organoid-derived tumor tissues

The direct 2.5D organoid-derived tumor tissues were histopathologically analyzed using H&E staining and immunohistochemical staining as described previously [9,12,19]. After the tissues were dissected, they were fixed with 4 % PFA for 24 h and embedded in paraffin. After deparaffinization, the slides were stained with H&E. Others underwent antigen retrieval in 10 mM citrate buffer at 121 °C for 5 min, and the endogenous peroxidase activity was stopped by treating the sections with 1 % peroxidase for 30 min. Thereafter, they were blocked with 1.5 % NGS/PBS for 30 min and were then incubated with primary antibodies (CK5; 1:200, CK7; 1:50, CK20; 1:200, UPK3A; 1:200, progesterone; 1:100, and TTF1; 1:100) and kept at 4 °C overnight followed by incubation with Dako Envision+dual Link System-HRP for 30 min. Slides were treated with a solution of ABC kit (Vector Laboratories, Burlingame, CA, USA) for 3–5 min. All images were obtained using a light microscope (BX-43; Olympus, Tokyo, Japan) and quantified using ImageJ densitometry analysis software.

2.10. Statistical analysis

The obtained data were presented as means ± S.E.M. Statistical analysis was done using the one-way analysis of variance (ANOVA) method followed by Bonferroni's test using Sigma Plot software (V 14.5, Systat Software Inc., CA, USA). When *P* values are < 0.05, the data were considered statistically significant.

3. Results

3.1. Generation of direct 2.5D organoids from different cancerous tissues

In the previous study, we established a novel culture method of dog 2.5D bladder cancer organoids using their parental 3D organoids and the special media called 2.5D media [19]. These 2.5D organoids recapitulated some characteristics of their parental 3D organoids such as marker expression, stemness, tumorigenesis, and drug sensitivity. In the present study, we hypothesized that 2.5D media are more suitable for culturing the primary cancer cells without losing their characteristics than 2D epithelial cell line media. To prove this hypothesis, various animal cancer cells were isolated from tissues, seeded at the same number of cells in the 2.5D media or normal DMEM media, and underwent various analyses (Fig. 1A). After seeding, various kinds of cancer cells showed better attachment and growth in the 2.5D media than in the normal DMEM media (Fig. 1B). The cells grown in the 2.5D media were successfully passaged several times, cryopreserved, and analyzed. These data indicate that 2.5D media could efficiently grow the tumor cells that were obtained directly from their original cancer tissues.

3.2. Cell proliferation speed in 2.5D media

We next examined the proliferation speed of six kinds of primary cancer cells cultured either in the 2.5D media or normal DMEM media (Fig. 2 and Supplementary Fig. 1). The cells seeded in the 2.5D media showed a significantly (statistical parameters are shown in Table 2) higher proliferation speed at day 1, 2, and 3 compared with the cells seeded in the normal DMEM media (Fig. 2A–G and Supplementary Fig. 1A-D). These data indicate that direct 2.5D organoids grow faster and we could shorten the time used in their analysis.

3.3. Cell marker expression in 2.5D media

To confirm if the cells grown in the 2.5D media consist of cancer cells, we performed immunofluorescence staining of the cells with different specific markers at early and late passages. Dog bladder cancer cells, mammary tumor cells, melanoma cells, and lung cancer cells expressed UPK3A, HER2, Melan A, and TTF1, respectively (Fig. 3A).

Table 5
Quantification of specific marker expression in 2.5D at high passage (>10).

UPK3A in BC cells				HER2 in canine mammary tumor cells				Melan A in dog melanoma cells				TTF1 in Dog lung cancer cells			
	Dapi	FITC	Positive cell (%)		Dapi	FITC	Positive cell (%)		Dapi	FITC	Positive cell (%)		Dapi	FITC	Positive cell (%)
Image 1	115	72	62.6087	Image 1	34	28	82.35294	Image 1	29	24	82.75862	Image 1	20	18	90.0
Image 2	80	62	77.5	Image 2	66	52	78.78788	Image 2	61	49	80.33	Image 2	19	17	89.5
Image 3	82	70	85.36585	Image 3	38	34	89.47368	Image 3	27	23	85.18519	Image 3	24	16	66.7
Average	92.33333	68.0	75.2	Average	46	38	83.5	Average	39.0	32.0	82.8	Average	21.0	17	82.0
SD	19.66	5.29	11.6	SD	17.44	12.49	5.4	SD	19.08	14.731	2.43	STDEV	2.6	1.00	13.32
S.E.M	11.35	3.06	6.67	S.E.M	10.07	7.21	3.14	S.E.M	11.015	8.505	1.40	S.E.M	1.5	0.6	7.69

Moreover, cat skin tumor cells and mammary tumor cells expressed CK5 and HER2, respectively (Fig. 3A). The quantification of the expression revealed that all cell strains expressed their specific markers at a high percentage (>80 %, Fig. 3B and Table 3). Interestingly, the 2.5D cells of dog bladder cancer and mammary tumors showed a significantly ($P \leq 0.005$, Table 4) higher expression of their specific markers compared with the cells grown in DMEM media (Supplementary Fig. 2A-F). Furthermore, in the late passage (>10), the 2.5D organoid cells maintained the expression of their specific markers (Supplementary Fig. 3A, B and Table 5). These data indicate that 2.5D media could maintain the cellular components of cancer cells even after late passage.

3.4. *Drug sensitivity of the cells cultured in 2.5D media*

To check the drug sensitivity of the cells cultured in 2.5D media, two strains of dog bladder cancer and dog mammary tumor 2.5D organoid cells as well as one strain of cat skin tumor, cat mammary tumor, dog lung cancer, and dog melanoma 2.5D organoid cells were evaluated (Fig. 4 and Supplementary Fig. 4). The cells showed different sensitivity profiles to anti-cancer drugs. For example, one bladder cancer strain showed resistance (IC50 >100 ng/ml), and the other showed a concentration-dependent sensitivity (IC50≤1 ng/ml) to mitoxantrone (Fig. 4A, B and Table 6). Also, these two strains exhibited a concentration-dependent and different sensitivity (different IC50) to vinblastine and carboplatin (Fig. 4A, B and Table 6). On the other hand, the two strains of dog mammary tumor cells showed a similar concentration-dependent and different sensitivity profile to doxorubicin, toceranib, and carboplatin (Fig. 4C and Table 6). The drug sensitivities of cat skin tumor, cat mammary tumor, dog lung cancer, and dog melanoma also revealed a concentration-dependent and different sensitivity to anti-cancer drugs (Supplementary Fig. 4 and Table 6). These data indicate that direct 2.5D organoids might be useful for rapid anti-cancer drug sensitivity tests.

3.5. *Tumorigenesis induced by the cells cultured in 2.5D media*

In the previous study, we demonstrated that 2.5D bladder cancer organoids derived from 3D organoids could form tumors *in vivo* and the formed tumor maintained the marker expression of their original tumor [19]. In the present study, we checked the tumorigenic potentials of the primary cultured cells in 2.5D media. After subcutaneous injection of dog bladder cancer, dog lung cancer, dog mammary tumor, or cat mammary tumor 2.5D organoid cells into the back of mice, xenografted tumors were successfully generated within 6 weeks (Fig. 5A, Supplementary Fig. 6A). The H&E staining of sections from the formed tumor tissues showed similar histopathology to their original tumor tissues (Fig. 5B). In case of BC, where the generated 2.5D organoid cells were derived from urine cells, the formed tumor tissue showed similar histopathology to BC histopathology (Supplementary Fig. 6B). To characterize the cellular components of the formed tumor tissues, immunohistochemical staining using each specific marker antibody was carried out. Expression of progesterone was observed in the dog mammary tumor 2.5 D organoid cell-derived tumor tissues as in their original tumor tissues (Fig. 5C). Expressions of TTF1 and CK5 were also observed in the lung tumor 2.5D organoid cells and cat mammary tumor 2.5D organoid cell-derived tumor tissues, respectively, as in their original tumor tissues (Fig. 5C, Supplementary Fig. 5, and Table 7). Expressions of UPK3A, CK20, and CK7 were also observed in the dog BC 2.5D organoid cells-derived xenografts (Supplementary Fig. 6C). These findings suggest that direct 2.5D organoids maintained the ability to form tumors *in vivo*.

4. Discussion

In the present study, we for the first time established a new culture method of direct 2.5D organoids using different kinds of cancer tissues

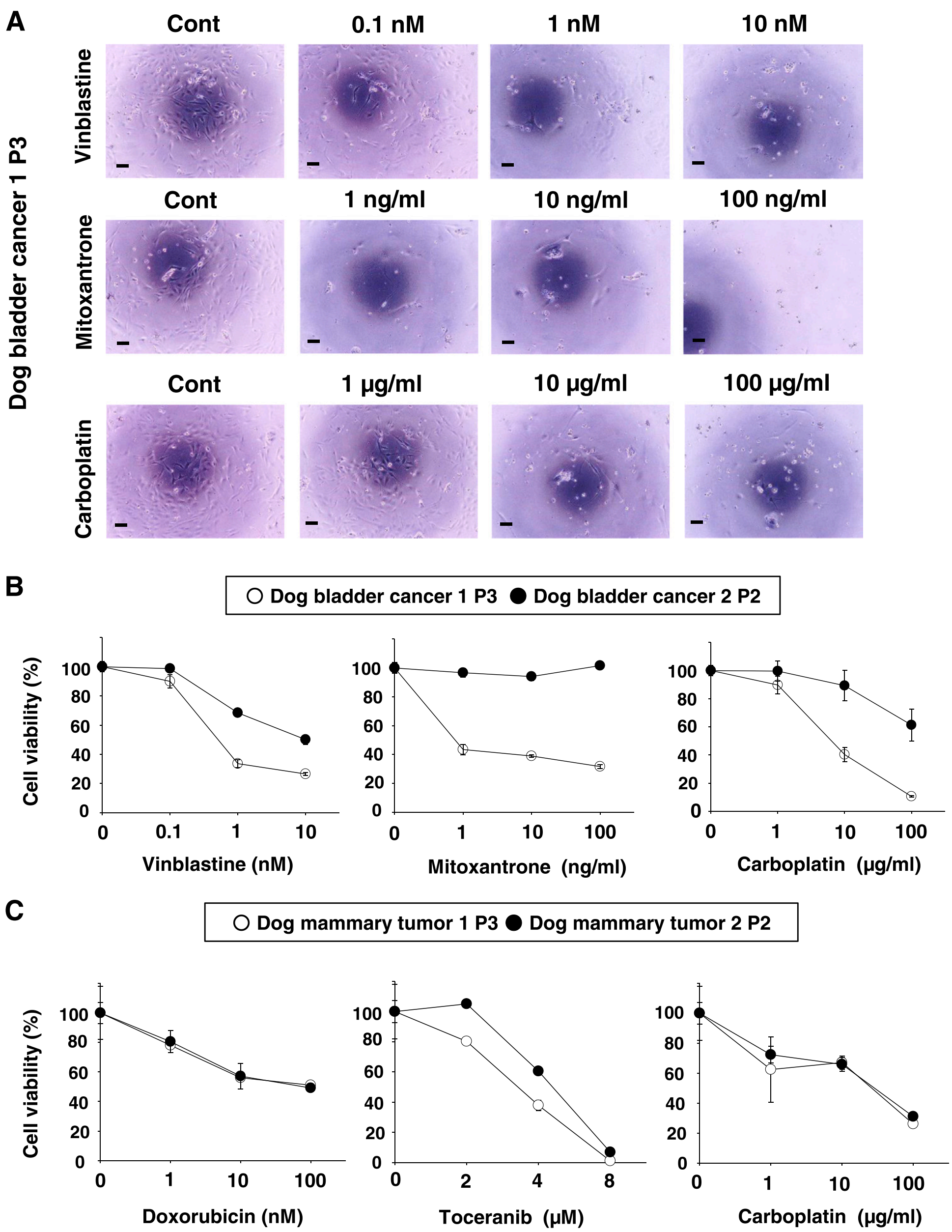

Fig. 4. Cell viability assay of the cells cultured in 2.5D media. After culturing the cells in 2.5D media, they were seeded on 96-well plates and treated with different concentrations of anti-cancer drugs for 72 h. Representative phase-contrast images of dog bladder cancer cells treated with different anti-cancer drugs are shown (A). Scale bar: 200 µm. Cell viability was evaluated using PrestoBlue kit (B, C, n = 6). The value 100 on Y-axis represents cell viability for each control and the data were expressed as mean ± S.E.M.

Table 6
Values of IC50 of different anticancer drugs for the different strains of direct 2.5D organoids.

Strains	Drug	IC50
Dog bladder cancer 1	Vinblastine	>10 nM
	Mitoxantrone	>100 ng/ml
	Carboplatin	>100 μg/ml
Dog bladder cancer 2	Vinblastine	0.511 nM
	Mitoxantrone	<1 ng/ml
	Carboplatin	6.37 μg/ml
Dog mammary tumor 1	Doxorubicin	>100 nM
	Toceranib	3.27 μM
	Carboplatin	28.6 μg/ml
Dog mammary tumor 2	Doxorubicin	77.7 ng/ml
	Toceranib	4.58 μM
	Carboplatin	26.1 μg/ml
Cat skin tumor 1	Toceranib	3.01 μM
	Carboplatin	31.9 μg/ml
Cat mammary tumor 1	Doxorubicin	>100 ng/ml
	Carboplatin	>100 μg/ml
Dog lung cancer 1	Cisplatin	65.2 μM
	Vinorelbine	0.079 μM
Dog melanoma 1	Toceranib	2.78 μM
	Carboplatin	19.5 μg/ml

from dogs and cats. These 2.5D organoids have maintained some characteristics of their parental tissues. The main findings of the present study are as follows: 1) direct 2.5D organoid cells were successfully isolated from the different strains of cancer tissues and urine by using our identified special 2.5D organoid media and showed a better attachment and growth compared with the 2D cell line media (Figs. 1), 2) the proliferation speed of direct 2.5D organoid cells was significantly higher in the 2.5D media than the normal DMEM media (Fig. 2 and Supplementary Fig. 1), 3) direct 2.5D organoids maintained expression of their specific cell markers even after late passages (Fig. 3 and Supplementary Fig. 3), 4) direct 2.5D organoids were usable for screening different anti-cancer drugs (Fig. 4 and Supplementary Fig. 4), 5) injection of direct 2.5D organoid cells into immunodeficient mice successfully generated tumors that were histopathologically similar to their original tissues (Fig. 5 and Supplementary Figs. 5, 6). Collectively, these data indicate that direct 2.5D organoids could be useful to investigate cancer biology and provide new insights for faster and more cost-effective precision veterinary medicine.

Most human cancer-related therapeutic studies depend on mouse models that scarcely translate into clinical success. Therefore, the naturally occurring cancers in companion animals, including dogs and cats that share most biological features with human cancers got more attention. Establishing dog and cat cancer models is valuable to comprehend the cancer biology of humans as they share most cellular and molecular characteristics such as histopathology, invasion, distant metastases, chemotherapy response, and prognosis [29–31]. In the previous study, we established a 3D organoid culture model of dog bladder cancer that recapitulated most biological features of human muscle-invasive bladder cancer [22]. From this model, we established a 2.5D bladder cancer organoid culture model that recapitulated most characteristics of their original 3D organoid model by using special 2.5D media [19].

In the present study, we established direct 2.5D organoids from different cancerous tissues of dogs and cats using special 2.5D media without a need for 3D organoids as in the previous study. After mincing and digesting the cancer tissues, the cells were seeded in the 2.5D media or 2D cell line media (normal DMEM supplemented with 10 % FBS and 1 % PS). Present cell cultures based on animal sera are not fully satisfactory especially for the *in vitro* expansion of cells intended for clinical applications [32]. The supplements in the 2.5D media helped the cells to attach, grow, and proliferate better than in the normal DMEM media (Fig. 1) since 2.5D media contain different vitamin and amino acid supplements such as Glutamax, nicotinamide, N-acetyl cysteine, HEPES, and transforming growth factor (TGF)-β, and A83–01. Several studies showed that these supplements improved the culture conditions of different cells. Supplementation with Glutamax revealed a positive influence on the proliferation and differentiation of male germ cells [33], mesenchymal stem cells from various tissues [34], and neural precursor cells [35] in vitro. This may be due to the Glutamax mainly supplementing the mammalian cells with their requirements of nitrogen used for nucleotides and nonessential amino acids and it is also used as a major energy source by cultured cells through glutaminolysis [36]. Using nicotinamide (source of oxidized nicotinamide adenine dinucleotide to suppress sirtuin activity [37]) and HEPES was necessary to improve the culture efficiency and extend the culture of the human small intestine and colon epithelial cells [38]. This may be due to the nicotinamide playing a critical role in cellular metabolism and maintaining mitochondrial homeostasis and genome integrity [39]. Moreover, A83-01 was added to prevent fibroblast proliferation [40]. N-acetyl cysteine was added as a cytoprotective antioxidant [41,42]. We, therefore, suggested that these culture supplements are important for generating the direct 2.5D cells from the primary tissues.

To further characterize bladder cancer 2.5D cells, we examined the cultured cells and xenografts using a UPK3A antibody (Fig. 3 and Supplementary Fig. 6C), which was used before to characterize uroepithelial cells in several studies [19,22,43–46]. Further, we used HER2 and CK5 antibodies to characterize dog mammary tumor epithelial 2.5D cells and cat mammary and skin tumor epithelial 2.5D cells by immunofluorescence, and used progesterone and CK5 antibodies to characterize dog mammary tumor and cat mammary tumor 2.5D cells-derived xenografts by immunohistochemistry (Figs. 3 and 5C). CK5 was used to characterize several dog mammary tumor cell lines [47–49], cat mammary tumor cells [50,51], and cat skin tumor epithelial cells [52,53]. We also used HER2 antibody to characterize cat mammary tumor cells as was before [51], Melan A antibody to characterize dog melanoma cells [54], and TTF1 antibody to characterize the canine lung adenocarcinoma cells [55]. In the current study, the 2.5D organoids maintained the expression of their specific markers even after high passages (Supplementary Fig. 3 A, B) and showed a significantly higher expression of these markers compared with cells grown in DMEM media (Supplementary Fig. 2A–F). Similarly, it was reported that cell marker expression and proliferative characteristics were significantly different in variable culture media [56,57]. Further, our established 2.5 organoid cells formed tumors successfully in SCID mice after injection. The histopathology of the formed tumor tissues demonstrated a similar structure to the original tissues where these cells were derived. These data indicated that our established cells mainly consist of tumor epithelial cells and possess the capacity of reproducing original tumor tissues.

Establishing patient-derived cancer cells directly from their tumor tissue samples in a short time is valuable and useful to find a suitable anti-cancer therapy. In the present study, we used our established direct 2.5D cells that recapitulated several characteristics of the original tumor samples to screen for several anti-cancer drugs (Fig. 4 and Supplementary Fig. 4). The cells showed concentration-dependent response to anti-cancer drugs, and different sensitivity profile was shown among the strains tested (Fig. 4 and Supplementary Fig. 4). There is a controversy in the drug sensitivities between 2D and 3D culture conditions. Due to the difference in the stemness conditions between them, drug sensitivity tends to be higher in the 2D model [58–60]. For example, in the mammary tumor, the dissimilarity in drug sensitivity among 2D and 3D cultures of several cell lines and primary cultured cells from a patient-derived xenograft and the patient's original tumor tissues was assessed [60]. The data revealed more resistance to doxorubicin and paclitaxel in the 3D organoids compared with the 2D cultured cells [60]. On the other hand, in the bladder cancer model, the effect of rapamycin and Bacillus Calmette-Guérin was higher in the 2D cell culture than that in the 3D organoids [61]. In our previous study, 3D-derived 2.5D organoid cells at early and late passages showed a similar sensitivity profile with parenteral 3D organoids indicating similar or close stemness

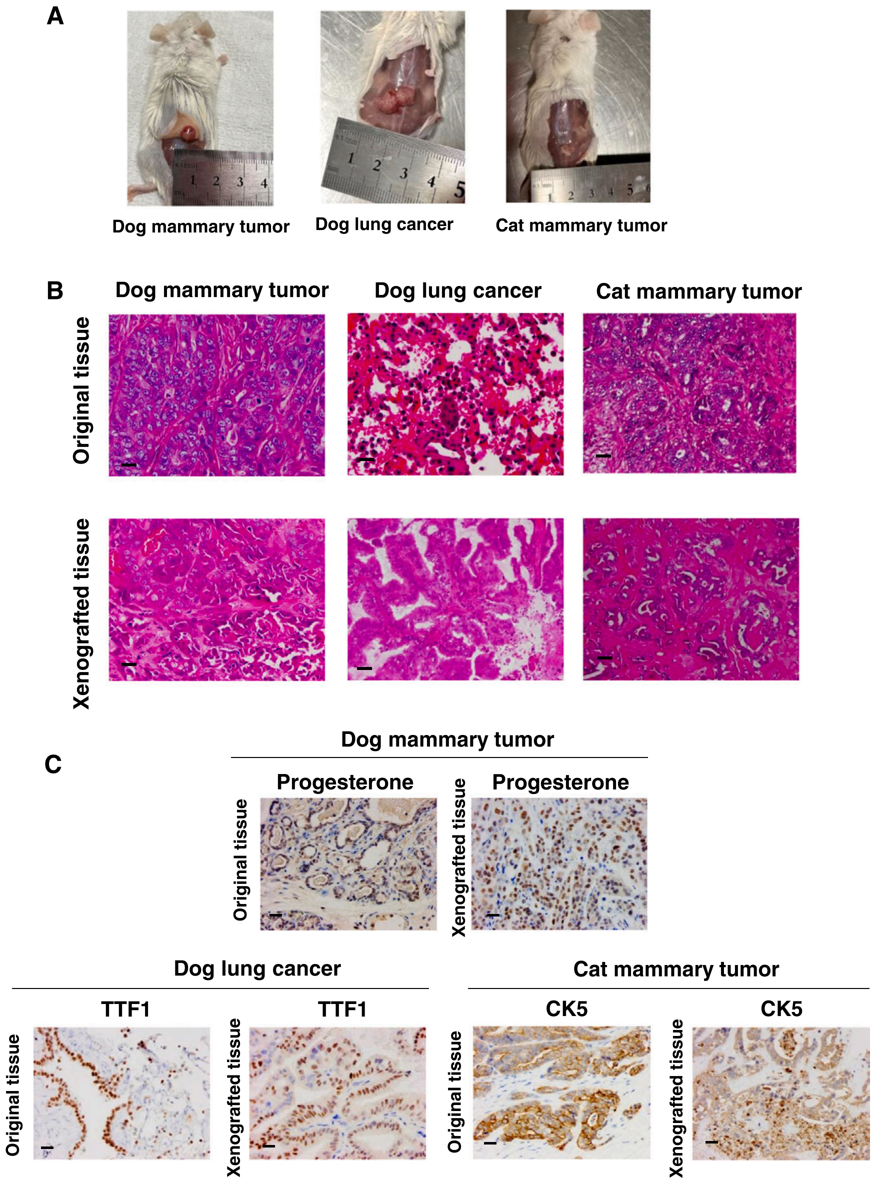

Fig. 5. Tumorigenic potentials of direct 2.5D organoid cells. Representative images of different tumors formed after injection with 1×10^6 direct 2.5D organoid cells per site (A). Representative comparative images of H&E-stained sections of the original tumor tissues and direct 2.5D organoid cell-xenografted tumor tissues are shown. Scale bar: 100 µm (B). Tissue marker expression in xenografted tissues. Expressions of progesterone, TTF1, and CK5 in dog mammary tumor, dog lung cancer, and cat mammary tumor 2.5D organoid cell xenografted tissues and the original tissues. Scale bar: 100 µm.

Table 7
Quantification of marker expression in different 2.5D cells after immunohistochemistry.

UPK3A in bladder cancer xenograft		CK20 in bladder cancer xenograft		CK7 in bladder cancer xenograft		TTF1 in Lung cancer tissue		TTF1 in Lung cancer Xenograft		CK5 in cat mammary tumor tissues		CK5 in cat mammary tumor xenogrft	
	Positive area (%)		Positive area (%)		Positive area (%)		Positive area (%)		Positive area (%)		Positive area (%)		Positive area (%)
Image 1	13.2	Image 1	3.2	Image 1	14.11	Image 1	10.45	Image 1	12.54	Image 1	25.22	Image 1	30.81
Image 2	10.14	Image 2	10.14	Image 2	9.8	Image 2	10.05	Image 2	16.26	Image 2	27.47	Image 2	24.15
Image 3	16.5	Image 3	16.5	Image 3	11.93	Image 3	7.48	Image 3	13.25	Image 3	27.9	Image 3	25.69
Average	13.28	Average	9.95	Average	11.95	Average	9.33	Average	14.02	Average	26.86	Average	26.88
SD	3.18	SD	6.65	SD	2.16	SD	1.61	SD	1.97	SD	1.44	SD	3.49
S.E.M	1.84	S.E.M	3.84	S.E.M	1.24	S.E.M	0.93	S.E.M	1.14	S.E.M	0.83	S.E.M	2.01

conditions between them [19]. Since we used the same components of 2.5D media to generate direct 2.5D organoids in the present study, these cells could be used efficiently for drug screening.

5. Conclusion

We for the first time generated a direct 2.5D organoid culture system from cancer tissues without the need for the 3D organoid system. Direct 2.5D organoids showed constant passages and higher proliferation speed in the 2.5D media compared with the normal 2D cell line media. Direct 2.5D organoids maintained the expression pattern of specific markers and demonstrated tumorigenesis *in vivo*. Furthermore, direct 2.5D organoids showed different responses to anti-cancer drugs among the different strains. These findings suggest that our established direct 2.5D culture method can be used as a cheaper, easier, and less-time consuming research model instead of 3D organoids to study cancer biology and to expedite precision veterinary medicine.

CRediT authorship contribution statement

All authors have approved submission of the manuscript and declare that no conflict of interest exists. **Amira Abugomaa, Mohamed Elbadawy, Haru Yamamoto** and **Hiromi Ayame, Yusuke Ishihara,** and **Yomogi Sato** performed pathological experiments. **Masahiro Kaneda** provided research sources and experimental tools. **Hideyuki Yamawaki** revised the manuscript. **Amira Abugomaa, Mohamed Elbadawy, Tatsuya Usui**, and **Kazuaki Sasaki** designed the study, analyzed, and interpreted the data, and wrote the manuscript.

Funding

This study was supported in part by JSPS KAKENHI Grant Number 22J11550.

Conflict of interest statement

The authors declare no competing financial and non-financial interests.

Data availability

No data was used for the research described in the article.

Appendix A. Supporting information

Supplementary data associated with this article can be found in the online version at doi:10.1016/j.biopha.2022.113597.

References

[1] P. Thumser-Henner, K.J. Nytko, C. Rohrer Bley, Mutations of BRCA2 in canine mammary tumors and their targeting potential in clinical therapy, BMC Vet. Res. 16 (1) (2020) 30.
[2] C.M. Fulkerson, D. Dhawan, T.L. Ratliff, N.M. Hahn, D.W. Knapp, Naturally occurring canine invasive urinary bladder cancer: a complementary animal model to improve the success rate in human clinical trials of new cancer drugs, Int. J. Genom. 2017 (2017) 6589529.
[3] H.L. Gardner, J.M. Fenger, C.A. London, Dogs as a model for cancer, Annu Rev. Anim. Biosci. 4 (2016) 199–222.
[4] H.M. Hayes Jr., K.L. Milne, C.P. Mandell, Epidemiological features of feline mammary carcinoma, Vet. Rec. 108 (22) (1981) 476–479.
[5] S.M. Prasad, G.J. Decastro, G.D. Steinberg, Medscape, urothelial carcinoma of the bladder: definition, treatment and future efforts, Nat. Rev. Urol. 8 (11) (2011) 631–642.
[6] J. Debnath, J.S. Brugge, Modelling glandular epithelial cancers in three-dimensional cultures, Nat. Rev. Cancer 5 (9) (2005) 675–688.
[7] A.F. Gazdar, V. Kurvari, A. Virmani, L. Gollahon, M. Sakaguchi, M. Westerfield, D. Kodagoda, V. Stasny, H.T. Cunningham, I.I. Wistuba, G. Tomlinson, V. Tonk, R. Ashfaq, A.M. Leitch, J.D. Minna, J.W. Shay, Characterization of paired tumor and non-tumor cell lines established from patients with breast cancer, Int J. Cancer 78 (6) (1998) 766–774.
[8] M.A. Lancaster, J.A. Knoblich, Organogenesis in a dish: modeling development and disease using organoid technologies, Science 345 (6194) (2014) 1247125.
[9] M. Elbadawy, M. Yamanaka, Y. Goto, K. Hayashi, R. Tsunedomi, S. Hazama, H. Nagano, T. Yoshida, M. Shibutani, R. Ichikawa, J. Nakahara, T. Omatsu, T. Mizutani, Y. Katayama, Y. Shinohara, A. Abugomaa, M. Kaneda, H. Yamawaki, T. Usui, K. Sasaki, Efficacy of primary liver organoid culture from different stages of non-alcoholic steatohepatitis (NASH) mouse model, Biomaterials 237 (2020), 119823.
[10] T. Takahashi, Organoids for drug discovery and personalized medicine, Annu Rev. Pharmacol. Toxicol. 59 (2019) 447–462.
[11] M. Elbadawy, Y. Sato, T. Mori, Y. Goto, K. Hayashi, M. Yamanaka, D. Azakami, T. Uchide, R. Fukushima, T. Yoshida, M. Shibutani, M. Kobayashi, Y. Shinohara, A. Abugomaa, M. Kaneda, H. Yamawaki, T. Usui, K. Sasaki, Anti-tumor effect of trametinib in bladder cancer organoid and the underlying mechanism, Cancer Biol. Ther. 22 (5–6) (2021) 357–371.
[12] M. Elbadawy, Y. Kato, N. Saito, K. Hayashi, A. Abugomaa, M. Kobayashi, T. Yoshida, M. Shibutani, M. Kaneda, H. Yamawaki, T. Mizutani, C.K. Lim, M. Saijo, K. Sasaki, T. Usui, T. Omatsu, Establishment of intestinal organoid from rousettus leschenaultii and the susceptibility to bat-associated viruses, SARS-CoV-2 and pteropine orthoreovirus, Int. J. Mol. Sci. 22 (19) (2021), 10763.
[13] M. Elbadawy, T. Usui, H. Yamawaki, K. Sasaki, Development of an experimental model for analyzing drug resistance in colorectal cancer, Cancers 10 (6) (2018), 164.
[14] A. Abugomaa, M. Elbadawy, H. Yamawaki, T. Usui, K. Sasaki, Emerging roles of cancer stem cells in bladder cancer progression, tumorigenesis, and resistance to chemotherapy: a potential therapeutic target for bladder cancer, Cells 9 (1) (2020), 235.
[15] T. Usui, M. Sakurai, K. Umata, M. Elbadawy, T. Ohama, H. Yamawaki, S. Hazama, H. Takenouchi, M. Nakajima, R. Tsunedomi, N. Suzuki, H. Nagano, K. Sato, M. Kaneda, K. Sasaki, Hedgehog signals mediate anti-cancer drug resistance in three-dimensional primary colorectal cancer organoid culture, Int. J. Mol. Sci. 19 (4) (2018), 1098.
[16] M. Elbadawy, A. Abugomaa, H. Yamawaki, T. Usui, K. Sasaki, Development of prostate cancer organoid culture models in basic medicine and translational research, Cancers 12 (4) (2020), 777.
[17] A. Elfadadny, H.M. El-Husseiny, A. Abugomaa, R.F. Ragab, E.A. Mady, M. Aboubakr, H. Samir, A.S. Mandour, A. El-Mleeh, A.H. El-Far, A.H. Abd El-Aziz, M. Elbadawy, Role of multidrug resistance-associated proteins in cancer therapeutics: past, present, and future perspectives, Environ. Sci. Pollut. Res. Int. 28 (36) (2021) 49447–49466.
[18] A. Abugomaa, M. Elbadawy, Patient-derived organoid analysis of drug resistance in precision medicine: is there a value? Expert Rev. Precis. Med. Drug Dev. 5 (1) (2020) 1–5.
[19] A. Abugomaa, M. Elbadawy, M. Yamanaka, Y. Goto, K. Hayashi, T. Mori, T. Uchide, D. Azakami, R. Fukushima, T. Yoshida, M. Shibutani, R. Yamashita, M. Kobayashi, H. Yamawaki, Y. Shinohara, M. Kaneda, T. Usui, K. Sasaki, Establishment of 2.5D organoid culture model using 3D bladder cancer organoid culture, Sci. Rep. 10 (2020), 9393.
[20] L. Puca, R. Bareja, D. Prandi, R. Shaw, M. Benelli, W.R. Karthaus, J. Hess, M. Sigouros, A. Donoghue, M. Kossai, D. Gao, J. Cyrta, V. Sailer, A. Vosoughi, C. Pauli, Y. Churakova, C. Cheung, L.D. Deonarine, T.J. McNary, R. Rosati, S. T. Tagawa, D.M. Nanus, J.M. Mosquera, C.L. Sawyers, Y. Chen, G. Inghirami, R. A. Rao, C. Grandori, O. Elemento, A. Sboner, F. Demichelis, M.A. Rubin, H. Beltran, Patient derived organoids to model rare prostate cancer phenotypes, Nat. Commun. 9 (1) (2018) 2404.
[21] E.R. Shamir, A.J. Ewald, Three-dimensional organotypic culture: experimental models of mammalian biology and disease, Nat. Rev. Mol. Cell Biol. 15 (10) (2014) 647–664.
[22] M. Elbadawy, T. Usui, T. Mori, R. Tsunedomi, S. Hazama, R. Nabeta, T. Uchide, R. Fukushima, T. Yoshida, M. Shibutani, T. Tanaka, S. Masuda, R. Okada, R. Ichikawa, T. Omatsu, T. Mizutani, Y. Katayama, S. Noguchi, S. Iwai, T. Nakagawa, Y. Shinohara, M. Kaneda, H. Yamawaki, K. Sasaki, Establishment of a novel experimental model for muscle-invasive bladder cancer using a dog bladder cancer organoid culture, Cancer Sci. 110 (9) (2019) 2806–2821.
[23] M. Elbadawy, K. Hayashi, H. Ayame, Y. Ishihara, A. Abugomaa, M. Shibutani, S. M. Hayashi, S. Hazama, H. Takenouchi, M. Nakajima, R. Tsunedomi, N. Suzuki, H. Nagano, Y. Shinohara, M. Kaneda, H. Yamawaki, T. Usui, K. Sasaki, Anti-cancer activity of amorphous curcumin preparation in patient-derived colorectal cancer organoids, Biomed. Pharmother. 142 (2021), 112043.
[24] R.C. Gaver, A.M. George, G.F. Duncan, A.D. Morris, G. Deeb, H.C. Faulkner, R. H. Farmen, The disposition of carboplatin in the beagle dog, Cancer Chemother. Pharmacol. 21 (3) (1988) 197–202.
[25] J.-X. Yin, Z. Wei, J.-J. Xu, Z.-Q. Sun, In vivo pharmacokinetic and tissue distribution investigation of sustained-release cisplatin implants in the normal esophageal submucosa of 12 beagle dogs, Cancer Chemother. Pharmacol. 76 (3) (2015) 525–536.
[26] X.J. Zhou, H. Landi, F. Breillout, R. Rahmani, Pharmacokinetics of navelbine after oral administration in the dog and the monkey, Anti-Cancer Drugs 4 (4) (1993) 511–515.
[27] M.F. Yancey, D.A. Merritt, S.P. Lesman, J.F. Boucher, G.M. Michels, Pharmacokinetic properties of toceranib phosphate (Palladia, SU11654), a novel tyrosine kinase inhibitor, in laboratory dogs and dogs with mast cell tumors, J. Vet. Pharmacol. Ther. 33 (2) (2010) 162–171.
[28] M. Elbadawy, K. Fujisaka, H. Yamamoto, R. Tsunedomi, H. Nagano, H. Ayame, Y. Ishihara, T. Mori, D. Azakami, T. Uchide, R. Fukushima, A. Abugomaa, M. Kaneda, H. Yamawaki, Y. Shinohara, T. Omatsu, T. Mizutani, T. Usui, K. Sasaki, Establishment of an experimental model of normal dog bladder organoid using a three-dimensional culture method, Biomed. Pharmacother. 151 (2022), 113105.
[29] D.W. Knapp, N.W. Glickman, D.B. Denicola, P.L. Bonney, T.L. Lin, L.T. Glickman, Naturally-occurring canine transitional cell carcinoma of the urinary bladder A relevant model of human invasive bladder cancer, Urol. Oncol. 5 (2) (2000) 47–59.
[30] D.W. Knapp, J.A. Ramos-Vara, G.E. Moore, D. Dhawan, P.L. Bonney, K.E. Young, Urinary bladder cancer in dogs, a naturally occurring model for cancer biology and drug development, ILAR J. 55 (1) (2014) 100–118.
[31] J.M. Wypij, A naturally occurring feline model of head and neck squamous cell carcinoma, Pathol. Res. Int. 2013 (2013), 502197.
[32] A. Muraglia, V.T. Nguyen, M. Nardini, M. Mogni, D. Coviello, B. Dozin, P. Strada, I. Baldelli, M. Formica, R. Cancedda, M. Mastrogiacomo, Culture medium supplements derived from human platelet and plasma: cell commitment and proliferation support, Front Bioeng. Biotechnol. 5 (2017) 66.
[33] A. Reda, H. Albalushi, S.C. Montalvo, M. Nurmio, Z. Sahin, M. Hou, N. Geijsen, J. Toppari, O. Soder, J.B. Stukenborg, Knock-out serum replacement and melatonin effects on germ cell differentiation in murine testicular explant cultures, Ann. Biomed. Eng. 45 (7) (2017) 1783–1794.

[34] A.Y. Lee, J. Lee, C.L. Kim, K.S. Lee, S.H. Lee, N.Y. Gu, J.M. Kim, B.C. Lee, O.J. Koo, J.Y. Song, S.H. Cha, Comparative studies on proliferation, molecular markers and differentiation potential of mesenchymal stem cells from various tissues (adipose, bone marrow, ear skin, abdominal skin, and lung) and maintenance of multipotency during serial passages in miniature pig, Res. Vet. Sci. 100 (2015) 115–124.
[35] H. Babu, J.H. Claasen, S. Kannan, A.E. Runker, T. Palmer, G. Kempermann, A protocol for isolation and enriched monolayer cultivation of neural precursor cells from mouse dentate gyrus, Front. Neurosci. 5 (2011) 89.
[36] S.S. Ozturk, B.O. Palsson, Growth, metabolic, and antibody production kinetics of hybridoma cell culture: 1. Analysis of data from controlled batch reactors, Biotechnol. Prog. 7 (6) (1991) 471–480.
[37] J.M. Denu, Vitamin B3 and sirtuin function, Trends Biochem. Sci. 30 (9) (2005) 479–483.
[38] T. Sato, D.E. Stange, M. Ferrante, R.G. Vries, J.H. Van Es, S. Van den Brink, W. J. Van Houdt, A. Pronk, J. Van Gorp, P.D. Siersema, H. Clevers, Long-term expansion of epithelial organoids from human colon, adenoma, adenocarcinoma, and Barrett's epithelium, Gastroenterology 141 (5) (2011) 1762–1772.
[39] E.F. Fang, S. Lautrup, Y. Hou, T.G. Demarest, D.L. Croteau, M.P. Mattson, V. A. Bohr, NAD(+) in aging: molecular mechanisms and translational implications, Trends Mol. Med. 23 (10) (2017) 899–916.
[40] M. Tojo, Y. Hamashima, A. Hanyu, T. Kajimoto, M. Saitoh, K. Miyazono, M. Node, T. Imamura, The ALK-5 inhibitor A-83-01 inhibits Smad signaling and epithelial-to-mesenchymal transition by transforming growth factor-beta, Cancer Sci. 96 (11) (2005) 791–800.
[41] M. Zafarullah, W.Q. Li, J. Sylvester, M. Ahmad, Molecular mechanisms of N-acetylcysteine actions, Cell Mol. Life Sci. 60 (1) (2003) 6–20.
[42] A. Kumar, L. Shalmanova, A. Hammad, S.E. Christmas, Induction of IL-8(CXCL8) and MCP-1(CCL2) with oxidative stress and its inhibition with N-acetyl cysteine (NAC) in cell culture model using HK-2 cell, Transpl. Immunol. 35 (2016) 40–46.
[43] K. Matsumoto, T. Satoh, A. Irie, J. Ishii, S. Kuwao, M. Iwamura, S. Baba, Loss expression of uroplakin III is associated with clinicopathologic features of aggressive bladder cancer, Urology 72 (2) (2008) 444–449.
[44] D. Zupancic, M. Zakrajsek, G. Zhou, R. Romih, Expression and localization of four uroplakins in urothelial preneoplastic lesions, Histochem Cell Biol. 136 (4) (2011) 491–500.
[45] J.A. Ramos-Vara, M.A. Miller, M. Boucher, A. Roudabush, G.C. Johnson, Immunohistochemical detection of uroplakin III, cytokeratin 7, and cytokeratin 20 in canine urothelial tumors, Vet. Pathol. 40 (1) (2003) 55–62.
[46] O. Kaufmann, J. Volmerig, M. Dietel, Uroplakin III is a highly specific and moderately sensitive immunohistochemical marker for primary and metastatic urothelial carcinomas, Am. J. Clin. Pathol. 113 (5) (2000) 683–687.
[47] C. Mei, L. Xin, Y. Liu, J. Lin, H. Xian, X. Zhang, W. Hu, Z. Xia, H. Wang, Y. Lyu, Establishment of a new cell line of canine mammary tumor CMT-1026, Front. Vet. Sci. 8 (2021), 744032.
[48] C. Perez-Martinez, M.J. Garcia-Iglesias, A.J. Duran-Navarrete, J. Espinosa-Alvarez, R.A. Garcia-Fernandez, N. Lorenzana-Robles, S. Fernandez-Perez, J.F. Garcia-Marin, Histopathological and immunohistochemical characteristics of two canine lipid-rich mammary carcinomas, J. Vet. Med. A Physiol. Pathol. Clin. Med. 52 (2) (2005) 61–66.
[49] L.N. Ramalho, A. Ribeiro-Silva, G.D. Cassali, S. Zucoloto, The expression of p63 and cytokeratin 5 in mixed tumors of the canine mammary gland provides new insights into the histogenesis of these neoplasms, Vet. Pathol. 43 (4) (2006) 424–429.
[50] D. Caliari, V. Zappulli, R. Rasotto, B. Cardazzo, F. Frassineti, M.H. Goldschmidt, M. Castagnaro, Triple-negative vimentin-positive heterogeneous feline mammary carcinomas as a potential comparative model for breast cancer, BMC Vet. Res. 10 (2014) 185.
[51] E. Dagher, J. Abadie, D. Loussouarn, D. Fanuel, M. Campone, F. Nguyen, Bcl-2 expression and prognostic significance in feline invasive mammary carcinomas: a retrospective observational study, BMC Vet. Res. 15 (1) (2019) 25.
[52] S. Ito, J.K. Chambers, C. Mori, A. Sumi, T. Omachi, H. Nakayama, K. Uchida, Comparative in vitro and in vivo studies on feline, canine, and human merkel cell carcinoma, Vet. Pathol. 58 (2) (2021) 276–287.
[53] F. Rodriguez Guisado, A. Suarez-Bonnet, G.A. Ramirez, Cutaneous spindle cell squamous cell carcinoma in cats: clinical, histological, and immunohistochemical study, Vet. Pathol. 58 (3) (2021) 503–507.
[54] M. Sforna, E. Chiaradia, I. Porcellato, S. Silvestri, G. Moretti, L. Mechelli, C. Brachelente, Characterization of Primary cultures of normal and neoplastic canine melanocytes, Animals 11 (3) (2021).
[55] J.A. Ramos-Vara, M.A. Miller, G.C. Johnson, Usefulness of thyroid transcription factor-1 immunohistochemical staining in the differential diagnosis of primary pulmonary tumors of dogs, Vet. Pathol. 42 (3) (2005) 315–320.
[56] W. Pustlauk, T.H. Westhoff, L. Claeys, T. Roch, S. Geißler, N. Babel, Induced osteogenic differentiation of human smooth muscle cells as a model of vascular calcification, Sci. Rep. 10 (1) (2020) 5951.
[57] S. Hagmann, B. Moradi, S. Frank, T. Dreher, P.W. Kämmerer, W. Richter, T. Gotterbarm, Different culture media affect growth characteristics, surface marker distribution and chondrogenic differentiation of human bone marrow-derived mesenchymal stromal cells, BMC Musculoskelet. Disord. 14 (1) (2013) 223.
[58] F. Deiss, A. Mazzeo, E. Hong, D.E. Ingber, R. Derda, G.M. Whitesides, Platform for high-throughput testing of the effect of soluble compounds on 3D cell cultures, Anal. Chem. 85 (17) (2013) 8085–8094.
[59] B. Weigelt, A.T. Lo, C.C. Park, J.W. Gray, M.J. Bissell, HER2 signaling pathway activation and response of breast cancer cells to HER2-targeting agents is dependent strongly on the 3D microenvironment, Breast Cancer Res. Treat. 122 (1) (2010) 35–43.
[60] Y. Imamura, T. Mukohara, Y. Shimono, Y. Funakoshi, N. Chayahara, M. Toyoda, N. Kiyota, S. Takao, S. Kono, T. Nakatsura, H. Minami, Comparison of 2D- and 3D-culture models as drug-testing platforms in breast cancer, Oncol. Rep. 33 (4) (2015) 1837–1843.
[61] M.J. Kim, B.H. Chi, J.J. Yoo, Y.M. Ju, Y.M. Whang, I.H. Chang, Structure establishment of three-dimensional (3D) cell culture printing model for bladder cancer, PLoS One 14 (10) (2019), e0223689.